RSC Advances

ROYAL SOCIETY OF CHEMISTRY

www.rsc.org/advances

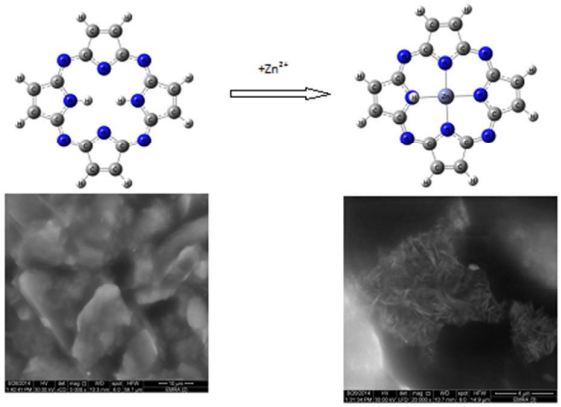

Naphthalocyanine derivative is incorporated in carbon paste electrode and examined as neutral carrier for Zinc selective electrode.

Potentiometric multi-walled carbon nanotube Zn-sensor based on naphthalocyanine neutral carrier: Experimental and theoretical studies

Ola R. Shehab*, Ahmed M Mansour

Chemistry Department, Faculty of Science, Cairo University, Gamaa Street, Giza 12613, Egypt

Abstract

A new multi-walled carbon nanotube graphite paste sensor based on 2,11,20,29-tetra-tert-butyl-2,3-naphthalocyanine as neutral carrier (2.0%), 2-flouorophenyl-2-nitrophenyl ether (50.0%) as plasticizer, and sodium tetrakis-imidazolyl borate (1.0%) as anionic additive has been explored as a selective sensor for determination of Zn^{2+} in real samples. The electrode showed a fast response time of 5 s, gave Nernstian response (29.9 mV/decade) over the concentration range 1.0×10^{-8}-1.5×10^{-4} molL^{-1}, and could be used in the pH range of 4.3-7.5 with a detection limit of 5.0×10^{-9} mol L^{-1}. The response mechanism of the electrode was investigated using UV-vis. and FT IR. Scanning electron microscope combined with energy dispersive X-ray spectrum were used to confirm the reaction between Zn^{2+} ions and naphthalocyanine on the surface of the electrode. In order to predict the selectivity of naphthalocyanine sensor for different metal ions, the corresponding binding energies of the metal complexes were calculated at Hartree-Fock level of theory.

Key Words: Naphthalocyanine; MWCNT; Zinc(II); NBO; HF

---

* Corresponding author, Tel.: +2 02 01001905350; Fax: +20 2 35728843. E-mail: olashehab_chem@yahoo.com

1. Introduction

Chemically modified carbon paste electrodes (CMCPEs) have been successfully applied as potentiometric sensors for determination of various species [1-4]. Compared to the other types of ion selective electrodes (ISEs), CMCPEs are extremely simple to prepare, easy to regenerate, and give stable response with a very low ohmic resistance [5,6] , corresponding to the formation of a very thin film of pasting liquid coated onto small particles of carbon powder [7]. Multi-walled carbon nanotubes (MWCNTs) were discovered by Iijima [8], which attracted great interest owing to its highly accessible surface area with a narrow distribution size, excellent electrical conductivity, and high stability. These properties encouraged analysts for using MWCNTs in the composition of sensors instead of normal graphite with a large particle size. The electrodes contained MWCNTs showed excellent features such as high sensitivity, low detection limit, and fast response that may be attributed to the signal enhancement provided by high surface area, low overvoltage, and rapid electrode kinetics [9]. Moreover, an improvement in the electric conductivity and mechanical properties of the paste matrix was reported.

In the present study, the choice of Zn(II) is ascribed for the presence of Zn(II) as a component of several enzymes such as carboanhydrases, and proteinases [10-12]. It is the second most abundant transition metal ion in the human body and plays significant role in many biological processes such as brain function and pathology, immune function, gene transcription. In addition, Zn(II) has unique ability to promote rewinding of the melted DNA, and can stimulate hydrolysis of DNA and RNA [13]. Zinc and its compounds are widely used in electroplating, paint, rubber, dye, wood preservatives, and batteries. However, its presence in high protein foods and its large doses can cause fever, chills, pulmonary manifestation, gastroenteritis, vomiting, nausea, anemia and renal failure. Besides, a major problem is the subsequent pollution and harm to the environment and humans because of its frequent use (Nolan et al. 2003[14]). For example, common zinc compounds such as zinc chloride, zinc oxide,

zinc sulfate and zinc sulfide are found at hazardous waste sites. In view of its toxicity, the determination of zinc(II) becomes more important. Several analytical techniques have been used for determination of Zn(II) such as flame atomic absorption spectrometry[15], fluorimetry [16], UV-vis.[17], ICP-AES [18], potentiometry [19-25], and voltammetry [26].

Macrocyles are most likely to be used in ISEs, however not all macrocyles are useful as sensing electrodes. They should provide high complexation or extraction selectivity for a particular metal ion and enough conformational flexibility for fast ion exchange. Besides that they must have high lipophilicity to remain in membrane and moderate molecular weight to allow high mobility. The function and applications of metallonaphthalocyanine coordination compounds are exciting as it expands from them being catalytic centers, through photosensitizing agents in therapy and other applications, to key cofactors in several biological systems. The selected macrocyclic ligand in this study (naphthalocyanine derivative) has attracting interest in the field of construction and design of new sensor capable of detecting definite metal ion of compatible dimensions in his electron rich heart cavity [27, 28]. Based on various parameters, the high stability and selectivity of its metal ion complex, its solubility and high ability to extract the metal ion into the paste phase, 2,11,20,29-tetra-tert-butyl-2,3-naphthalocyanine was explored as an active material in carbon paste electrode for the fabrication of Zn^{2+} selective sensor. Comparison between the proposed electrode and the reported Zn^{2+} sensors based on macrocyclic ionophores [27-35] 49-55] showed that the developed sensor has superiority over the reported electrodes in terms of low detection limit and high response time (Table 1).

2. Experimental

2.1. Chemicals

Graphite powder, 2,11,20,29-tetra-tert-butyl-2,3-naphthalocyanine**,** sodium tetraphenylborate (NaTPB), sodium tetrakis[3,5-bis(trifluoromethyl)phenyl]borate (NaTFPB), sodium tetrakis imidzolyl borate

(NaTImB), dibutyl-butyl phosphonate (DBBP), o-nitrophenyloctyl ether (o-NPOE), dioctyl adipate (DOA), tricresyl phosphate (TCP), 2-flouorophenyl-2-nitrophenyl ether (FPNPE), and THF were purchased from Aldrich chemical company. MWCNT (3-20 nm OD, 1-3 nm ID, 0.1-10 micro long) was purchased from Alfa Aesar. $NaNO_3$, KNO_3, NH_4NO_3, $Cd(NO_3)_2$, $Ba(NO_3)_2$, $Ni(NO_3)_2.6H_2O$, $Pb(NO_3)_2$, $Mg(NO_3)_2 \cdot 6H_2O$, $Mn(NO_3)_2 \cdot 4H_2O$, $Al(NO_3)_3 \cdot 9H_2O$, $Cu(NO_3)_2 \cdot 3H_2O$, and $Ca(NO_3)_2 \cdot 4H_2O$ were purchased from Oxford, India.

2.2. Apparatus

Digital Jenway 3010, and 3505 pH meters were used for potential, pH measurements, respectively. A SENTEK R1/2MM Ag/AgCl electrode was used as the outer reference electrode. UV/Vis spectra were recorded on a Shimdazu Lambda 4B spectrophotometer. FT IR-460 plus JASCO 4000-400 cm^{-1} was used for IR measurements (KBr pellets & solutions in THF). Perkin-Elmer Optima 2000 ICP instrument was used for the atomic emission spectrometry measurements. Quanta FEG 250 instrument was used to obtain the scanning electron micrographs (SEM) of the electrodes.

2.3. Sensors preparation

The modified paste was prepared by mixing the appropriate weight of naphthalocyanine, and highly pure graphite with acetone. The mixture is homogenized by careful mixing with agate pestle in agate mortar, left at room temperature to evaporate acetone, and then a weighed amount of the plasticizer is added. Similar, the MWCNT sensor was prepared by the same way with the addition of the MWCNT to the graphite powder. The paste is then packed into the electrode body [36]. All EMF measurements were carried out with the following cell assembly:

Ag//AgCl, KCl (3 M) // test solution //filling graphite modified paste // carbon paste electrode

2.4. Selectivity of the sensor

Potentiometric selectivity factor ($K_{A,B}^{Pot}$) was evaluated using the separate solution method (SSM) [37] according to the following relation:

$$\log K_{A,B}^{Pot} = \frac{E_B - E_A}{S} + (1 - \frac{Z_A}{Z_B})\log a_A$$

where E_A, E_B are the electrode potentials of 1.0×10^{-3} mol L^{-1} solution of each of Zn^{2+} and interfering cation, Z_A, Z_B are the charges on Zn^{2+} and the interfering cations, respectively and S is the theoretical slope.

2.5. Potentiometric determination

Standard addition method was applied for the potentiometric determination [38]. In this method, known amounts of standard Zn^{2+} were added to a sample of 25.0 ml with the unknown concentration and from the potential change, $\Delta E = (E_u - E_s)$ one can determine the concentration of the test sample using the equation:

$$C_x = C_s \left(\frac{V_s}{V_x + V_s}\right) \left(10^{(\Delta E/S)} - \frac{V_x}{V_s + V_x}\right)^{-1}$$

where: C_x is the unknown concentration, V_x is the volume of sample solution, V_s and C_s are the volume and concentration of the standard Zn^{2+} solution added to the sample, respectively, ΔE is the change in potential after addition of certain volume of standard solution, and S is the slope of the calibration graph.

2.6. Computational details

Full-unconstrained geometry optimization of 2,11,20,29-tetra-tert-butyl-2,3-naphthalocyanine and its complexes have been carried out at Hartree-Fock (HF) level of theory. In the model structures of naphthalocyanine, the naphthalene and tertiary butyl groups were replaced by H atoms [36] to reduce the computer time. The standard 6-31G(d) basis set was used for Na^+, Mg^{2+}, Al^{3+}, K^+, Ca^{2+}, Mn^{2+}, Ni^{2+}, Cu^{2+}, and Zn^{2+}, while the effective-core potential (ECP) of LANL2DZ was applied for Cd^{2+}, Ba^{2+} and

Pb^{2+}. The effect of solvent on the theoretical parameters was performed using the default Polarized Continuum Model (PCM) [39], where water as a solvent was considered as a uniform medium (ε = 78.39). Ionization energy, electron affinity, hardness, softness, dipole moment, and energy gap were calculated according to Koopman's theorem [40]. Natural bonding orbitals (NBO) analysis [41] of Mn^{2+}, Ni^{2+}, Cu^{2+}, and Zn^{2+} complexes were performed using NBO 3.1 program at the HF/6-31G(d) level of theory. All the calculations were carried out by Gaussian 03 package [42].

3. Results and Discussion

3.1. Factors affecting the performance of the Zn(II) sensor

3.1.1. Effect of Composition

It is well known that the performance characteristics (sensitivity, selectively, detection limit, and linear range) depend on the properties of the plasticizer, graphite/plasticizer ratio, and the nature and the amount of the ionophore [43]. In the present study, the influence of the amount of naphthalocyanine as an ionophore on the potential response of the developed CMCP electrode as a function of the zinc activity was investigated in the concentration range from 1.0×10^{-8} to 1.0×10^{-3} mol L^{-1}. As shown in Table 2, the electrodes containing only 2 and 3% of the ionophore exhibited super Nernstian response towards Zn^{2+} ions with slopes of 43.0, 55.0 mV/concentration decade, narrow linear ranges of 2.5×10^{-4}-5.0×10^{-3}, 3.2×10^{-4}-3.2×10^{-3} mol L^{-1} and high detection limits of 1.6×10^{-4}, 1.0×10^{-4} mol L^{-1}, respectively. To enhance the performance characteristics of the present sensors, other paste components such as cationic/anionic additive, type and amount of plasticizers, etc. needed to incorporate and study [44-46]. It was found that the electrode dipped with NaTFPB as anionic additive showed better performance in terms of slope, detection limit, and linear range. For example, the slope of the electrode No. 4 comes closer to the Nernstian (33.2 mV) with a wider linear range of 3.9×10^{-6}-5.0×10^{-3} mol L^{-1} and the detection limit is decreased to 3.8×10^{-6} mol L^{-1} comparing with the non-dipped one. While the incorporation of CTAB as cationic additive into the modified paste diminishes the slope of the sensor

which makes it not applicable. Then, the effect of the amount of naphthalocyanine was studied in presence of NaTFPB as anionic additive aiming to obtain superior performance. The results (Table 2) indicated that the optimum behavior was obtained by using 2% (w/w) of the ionophore. Further increase in the amount of the ionophore led to an increase in the slope and the detection limit of the sensor. By using the same mass percentage of the ionophore and changing the type of the additive from NaTFPB to NaTPB or NaTImB, it can be seen that the electrode dipped with NaTImB (Table 2, No 6) gave better Nernestian response (29.9 mV) and detection limit of 2.13×10^{-6} mol L^{-1} comparing with the other studied anionic additives.

Since the use of plasticizers gives some permeable properties to the paste and may improve the mechanical stability of the sensor [47], so it was necessary to study the response characteristics of the electrode in terms of the nature of plasticizer [43, 48, 49]. For this, different types of plasticizers, NPOE (ε = 23.6), DBP (ε = 6.4), DOA (ε =3.9), TCP (ε = 6.9), DBBP (ε = 4.6), and FPNPE (ε = 50.0) were examined. As shown in Table 2, the best performance was observed for the electrodes plasticized with NPOE and FPNPE with slopes 29.9, and 29.3 mV, in that order. The highest dielectric constant of FPNPE may be the main reason for decreasing the detection limit of the investigated electrode to 2.0×10^{-7} mol L^{-1}. Therefore, FPNPE was chosen as the best plasticizer for the working electrode. Alternatively, highly accessible surface area with a narrow distribution size, excellent electrical conductivity, and high stability of MWCNT attract the authors to explore the performance of the naphthalocyanine electrode in terms of different amount of the added MWCNT. As shown in Table 2 (No. 16) and represented in Fig. 1, the electrode doped with 1% MWCNT showed great enhanced sensitivity observed by the lower detection limit, 5.0×10^{-9} mol L^{-1} compared with its analogue without MWCNT (no.14).

3.1.2. Effect of pH

In order to examine the pH effect on the potential response of the electrode, the potential values for the Zn^{2+} solutions containing concentrations of 10^{-2}-10^{-4} mol L^{-1} and having different pH values were measured. The pH value from 1.0 to 10.0 was adjusted by adding diluted solutions of HNO_3 or NaOH. The potential change as a function of pH is plotted in Fig. 2. The obtained data showed that the working pH range is 4.3-7.5. In alkaline medium, the possibility for the formation of $Zn(OH)_2$ is present and below pH = 4.3, the change in the potential may be due to the protonation of the naphthalocyanine molecule, which will decrease its tendency to complex formation.

3.1.3. Response time

The response time of the electrodes was measured after the successive immersion of the electrodes in a series of Zn^{2+} solutions. In each solution, the Zn^{2+} concentration increased tenfold from 1.0×10^{-7}-1.0×10^{-3} molL^{-1} and 1.0×10^{-8}-1.0×10^{-4} mol L^{-1} for electrodes No. 14 (without 1% MWCNT) and 16 (with 1% MWCNT). Comparison between the two pastes (Fig. 3) revealed that sensor No. 16 reaches the equilibrium potential (5 s) faster than the other (11 s). This indicates a rapid diffusion achievement of the equilibrium between the aqueous layer and the carbon paste phase, rapid complex formation, and exchange of ions.

3.1.4. Effect of Temperature

The thermal stability of the sensors, calibration graphs (electrode potential vs. $p_{Zn^{2+}}$) were measured in the temperature ranges of 25-50 ºC (Table 3). The isothermal coefficient (dE°_{cell}/dt) was determined from the linear relation between E°_{cell} and temperature (t-25) as a slope (Fig. 4), where t is the experimental temperature [50]. The values of the standard cell potential E°_{cell} were obtained from the calibration plots as the intercept of these plots at $p_{Zn^{2+}} = 0$, and then were added to the standard electrode potential of the Ag/AgCl reference electrode at different temperatures to calculate the standard electrode (Zn-CMCPE) potentials ($E°_{elec}$). The values of dE°_{cell}/dt were found to be 2.11×10^{-3}, and 4.66×10^{-4} V/ºC, while the values of dE°_{elect}/dt were 1.345×10^{-3}, and 1.23×10^{-3} V/ºC for the sensors

without and with 1% MWCNT, respectively. The obtained results exhibited fairly high thermal stability of the studied sensors within the investigated temperature range with no deviation from the Nernstian behavior.

3.1.5. Selectivity of electrodes

The selectivity coefficient is the main source of information concerning interferences on the electrode response and is defined by its relative response to the primary ion over the other ions present in the solution [51]. Potentiometric selectivity coefficients were measured by the separate solution method (SSM) [37]. The values of the selectivity coefficients for electrodes No. 14 and 16 are given in Table 5. For electrode No. 14, all the selectivity values are < 1 except for Al^{3+}, while the values of all the interfering cations in case of sensor No. 16 (with 1% MWCNT) are less than one, indicating that these cations have negligible disturbance on the functioning of the investigated electrodes, and the enhancement of the selectivity pattern observed by adding the MWCNT.

3.2. Response mechanism

The mechanism of the investigated Zn^{2+} sensor was explored by observing the electronic absorption spectra of the naphthalocyanine ionophore in THF before and after the reaction with 0.1 M Zn^{2+} solution. Porphyrins are characterized by intense and sharp absorption bands in the range of 400-500 nm referred as Soret or B-band. In the range of 500-700 nm, the electronic spectra of porphyrins and their naphthalocyanine derivatives show a group of bands named Q-bands [42]. The electronic absorption spectrum of the titled ionophore displayed several bands in the UV-region at 210, 245, 280, 325, and 360 nm as well as a shoulder at 405 nm. Besides, a strong band at 780 nm and two shoulders at 695 and 735 nm are observed in the visible range (Fig. 5). By adding Zn^{2+} ions to the naphthalocyanine solution, a clean renovation to new species was observed as evidenced by a blue shifted of the Q-band to 760 nm and the disappearance of the band at 360 nm. Another attempt to investigate the mechanism of the electrode towards Zn^{2+} was obtained using solution FT IR analysis (in

THF). The IR spectrum of the free ionophore (Fig. 6(A)) showed a medium band at 1628 cm^{-1} assigned to ν(C=N). This mode was shifted to lower wave number and overlapped with the C=C vibrational modes in the same region with the appearance of the band at 1563 cm^{-1}. Therefore, the C=N groups are involved in chelation (Fig. 6(B)). Assignment of the NH group before and after adding Zn^{2+} ions to naphthalocyanine solution is not easy owing to presence of H-bonds between ionophore and THF molecules. For this, the spectrum of the paste containing the ionophore, graphite, FPNPE, and NaTImB was compared to the spectrum of the same paste after keeping in contact with 0.1 M Zn^{2+} for 1h and then rinsed with water for 10 s. Comparison between the solid spectra indicated that NH groups are involved in complexation formation as the ν(NH) mode is shifted from 3425 to 3416 cm^{-1} upon contact with Zn^{2+}. Therefore, naphthalocyanine interacted with Zn^{2+} as a neutral carrier through four coordination centers.

Scanning electron microscope (SEM) is a valuable tool used for characterizing the surface morphology of the sensor. As shown in Fig. 7, the appearance of the metallic zinc on the surface of the sensor having the titled ionophore after its dipping in a solution of Zn^{2+} for one hour could be taken as evidence for the surface reaction. Energy dispersive X-ray (EDX) is a key tool used for identification of sample, since each element has a unique atomic structure that allow unique set of peaks on its X-ray spectrum. The growing of a sharp and intense peak for zinc at about 8.6 KeV in the EDX spectrum of the surface of the electrode after dipping in zinc solution (Fig. 7) is a sign for the successful reaction of the titled ionophore with the Zn^{2+} ions at the electrode surface.

3.3. Quantum chemical calculations

The most essential property for metal ion selectively with naphthalocyanine is the binding energy (B.E.). Binding energies are defined as the total energy of complex minus the sum of total energies of the most stable isolated moieties, i.e., metal ion, and free naphthalocyanine. The energies of the free metal ions and naphthalocyanine have been calculated in the aqueous phase at Hartree-Fock (HF) level

of theory. The standard 6-31G(d) basis set was used for Na^+, Mg^{2+}, Al^{3+}, K^+, Ca^{2+}, Mn^{2+}, Ni^{2+}, Cu^{2+}, and Zn^{2+}, while LANL2DZ was applied for Cd^{2+}, Ba^{2+} and Pb^{2+}. The calculated values of binding energies are given in Table 5. The binding energies sequences follow the order $Ba^{2+} > Pb^{2+} > Cd^{2+} > K^+ > Ca^{2+} > Al^{3+} > Na^+ > Zn^{2+} > Mg^{2+} > Mn^{2+} > Cu^{2+} > Ni^{2+}$. The titled ionophore has a large flexible cavity, which can accommodate a variety of metal ions to form stable coordination compounds. The interference coming from the stable isoelectronic configurations of neon (Na^+ and Al^{3+}), argon (K^+ and Ca^{2+}), and xenon (Ba^{2+}), Cd^{2+} ([Kr]$4d^{10}$), as well as Pb^{2+} ([Xe]$4f^{14}5d^{10}6s^26p^2$) might be attributed to several explanations. First, it is necessary to clarify that our calculations were performed on a single molecule in the aqueous phase, rather than the experimental measurements which were carried out on the bulk solution. Second, the solvent properties such as hydrogen-bond ability and solute-solvent interactions cannot be provided by PCM model and these variables are well known to affect the selectivity of the titled ionophore, and also the value of formation constant. The stereochemistry of the formed metal complexes may be one of the reasons which did not be considered in the calculations as our assumption was based on the formation of square-planar geometry. In quantum chemical calculations, it is difficult to take into consideration several variables such as the complexity of the paste (additives, plasticizer, etc) and electrode-solution interface. Finally, the energies values of the free interfering cations were found to be lower than Zn^{2+} ion, while the corresponding complexes have higher energies than the zinc ionophore complex, despite these ions have little ability towards the formation of metal complexes owing to the absence of incomplete d-orbitals.

Natural bond orbital (NBO) analysis was carried out for the complexes of Mn, Ni, Cu, and Zn to shed more light about the preference of the investigated naphthalocyanine towards Zn among the transition metal ions. NBO can provide details about the type of hybridization, the nature of bonding and strength of the interactions between metal ion and donor sites [41]. According to NBO, the electronic configurations of Mn, Ni, and Cu in naphthalocyanine complexes are [Ar]$4s^{0.13}3d^{5.20}4p^{0.19}$,

$[Ar]4s^{0.25}3d^{8.15}4p^{0.25}$, and $[Ar]4s^{0.29}3d^{9.75}4p^{0.21}$ comparing with $[Ar]4s^{0.25}3d^{9.95}4p^{0.27}$ for the Zn complex. The calculated natural charges were found to be 1.478e, 1.346e, 0.752e, and 1.528e for Mn, Ni, Cu, and Zn in that order. The quantity of electron density donation from the donor sites of the ionophore to the metal ions is not the same. The natural charges are more reduced in case of Ni and Cu comparing with Mn and Zn as the half- and completely filled d-orbitals, which give extra stability to these complexes. The increase in the binding energy of Zn^{2+} with respect to the other transition metal elements may be assigned to the back donation from the completely filled d-orbitals to the empty p-orbitals in the titled ionophore.

The energies and compositions of the frontier molecular orbitals [53] are important properties in several chemical and pharmacological processes. E_{HOMO} is associated with the electron donating ability, while E_{LUMO} indicates the ability of the molecule to accept electrons. The chemical hardness and softness of a molecule as good indicator for the chemical reactivity of a given molecule can be calculated from the energy values of E_{HOMO} and E_{LUMO}. HOMO-LUMO gap (ΔE) decides whether the molecule is hard or soft; a soft molecule is more polarizable than the hard one. Hard molecules need small energy to excitation. Softness (*S*) is a property of molecule that measures the extent of chemical reactivity. It was found that Mn, Ni, Cu, and Cd complexes are harder than Zn(II) complex. Dipole moment (μ in Debye) was used to qualitatively analyze the trend in the hydrophobic values (Log P). A very significant dipole moment may polarize the molecule in such a way that it produces a required potential at several atomic centers necessary for binding and activity. Herein, the higher dipole moment values were reported for Pb, Al, Ca, and Zn in that order. Fig. 8 shows the optimized structures of free ionophore, and Zinc-ionophore complex; HOMO and LUMO of zinc -ionophore complex.

3.4. Analytical Applications

3.4.1. Real Samples Analyses

The Zn(II)-MWCNT-CPE was successfully used for the determination of Zn^{2+} ions in the real samples. For example, one gram of Mamy-vit, as a multivitamin drug (APEX pharma S.A.E.), supplied from a mixture of ten capsules was dissolved in 5 mL of concentrated nitric acid and digested to dryness. Then 3 mL more of nitric acid was added to the dry beaker and the pH was adjusted to the desired pH of the investigated sensor, further by dilution with water to 500 mL [54]. Another real sample was obtained from Prisoline zinc eye drop (Khaira pharma and chem. InD). The working sample was prepared by diluting a volume of 10 mL to 100 mL with water. Furthermore, different water samples were analyzed coming from tap water, chemical laboratory, and from granite factory. The pH of these samples was adjusted. The concentration of Zn^{2+} ions was measured by the proposed Zn(II)-MWCNT-CPE and atomic absorption spectrometry (AAS) for comparison. As shown in Table 6, a superior agreement between the two methods as confirmed by the high recovery values (97.8-102.4%) and the low RSD% values.

3.4.2. Potentiometric titrations

Zn(II) ions can be titrated with potassium ferrocyanide according to the following equation [55],

$$2K_4[Fe(CN)_6] + 3Zn(NO_3)_2 = K_2Zn_3[Fe(CN)_6]_2 + 6KNO_3$$

where Zn(II)-MWCNT-CMCPE was used as an indicator. In this titration, 10 and 15 mL of 1×10^{-4} mol L^{-1} Zn^{2+} and 10, 15, 20 mL of 1×10^{-3} mol L^{-1} Zn^{2+} and 10, 15 mL 1×10^{-2} mol L^{-1} Zn^{2+} solution were titrated against 1×10^{-4}, 1×10^{-3}, and 1×10^{-2} mol L^{-1} ferrocyanide solutions, respectively (Fig. 9). The obtained results revealed that the potential difference of the electrode is increased upon the addition of the ferrocyanide solution with the detection of a sharp end-point. The data (Table 7) shows the accuracy and reproducibility of the electrode.

3.5. Validation of the proposed electrode

The reproducibility and stability of the electrode were investigated by repeating the preparation and the calibration of each composition four times. As shown in Table 1, the RSD% values were found

to be in the range of 0.21-2.56%. The potential readings for the electrode No. 16 dipped in 1.0×10^{-4} mol L^{-1} Zn^{2+} solution ten times are negligibly changed (±0.5 mV) over 4h, which indicates the good reproducibility and high stability of the electrode. The accuracy was expressed in terms of percentage deviation of the measured concentration from the actual concentration. The obtained results (Table 6) are within the acceptance range of 3%.

The ruggedness of the potentiometric method was carried out by constructing the calibration curve using the same working solution, electrode, and experimental conditions over four days, and with four different persons. The RSD% values were found to be less than 1% for the repetitive experiments in four days, and < 2% for the repetitive experiments by the different workers. The obtained data revealed that the method is reproducible.

4. Conclusion

2,11,20,29-tetra-tert-butyl-2,3-naphthalocyanine as a neutral carrier contained in a modified carbon paste electrode has been used for the determination of Zn(II) ions (in the nano-molar levels) in the real samples such as multivitamin drug, Prisoline zinc eye drop and water samples (chemical laboratory and granite factory). Addition of a multi-walled carbon nanotube (MWCNT) to this electrode resulted in a great enhanced sensitivity observed by the lower detection limit, 5.0×10^{-9} mol L^{-1}. Besides, this sensor has higher electrical conductivity and higher resistance to interferents. High sensitivity, and selectivity, a wide range, a low detection limit, and very fast response time are the significant properties of the investigated electrodes. The increase in the binding energy of Zn^{2+} with respect to the other transition metal elements may be assigned to the back donation from the completely filled d-orbitals to the empty p-orbitals in the titled ionophore.

References

[1] A. Abbaspour , S.M.M. Moosavi, Chemically modified carbon paste electrode for determination of copper(II) by potentiometric method, Talanta 56 (2002) 91-96.

[2] H.M. Abu-Shawish, S.M. Saadeh, A New Chemically Modified Carbon Paste Electrode for Determination of Copper Based on N,N' Disalicylidenehexameythyl-enediaminate Copper(II) Complex, Sensor lett 5 (2007) 565-571.

[3] K. Kalcher, J.M. Kauffmann, J. Wang, I. Svancara, K. Vytras, C. Neuhold, Z. Yang, Sensors Based on Carbon Paste in Electrochemical Analysis: A Review with Particular Emphasis on the Period 1990-1993, Electroanalysis 7 (1995) 5-22.

[4] J. Pei, Q. Yin**, J.** Zhong, Potentiometric determination of trace silver based on the use of a carbon paste electrode, Talanta 38 (1991) 1185-1189.

[5] I. Svancara, K. Schachi, Testing of umodified carbon paste electrodes, Chem. Listy 93 (1999) 490-499.

[6] K. Vytras, J. Kalous, J. Jezkova, Automated potentiometry as an ecologic alternative to twophase titrations of surfactants, Egypt J. Anal. Chem. 6 (1997) 107-123.

[7] I. Svancara, M.K. Hvizdalova , K. Vytras, K. Kalcher, R. Novotny, A microscopic study on carbon paste electrodes, Electroanalysis 8 (1996) 61-65.

[8] S. Iijima, Helical microtubules of graphitic carbon, Nature 354 (1991) 56-58.

[9] M.M. Ardakani, M.A. Sheikh-Mohseni, Carbon Nanotubes - Growth and Applications; M. Naraghi, InTech. (2011).

[10] Y.H. Chiu, G.J.Gabriel, J.W. Canary, Ternary ligand-zinc-hydroxamate complexes, Inorg. Chem. 44 (2005) 40-44

[11] T.A. Miller, D.J. Witter, S.J. Belvedere, S. Histone deacetylase inhibitors, J. Med. Chem. 46 (2003) 5097-5116.

[12] A. Scozzafava, C.J. Supuran, Carbonic anhydrase and matrix metalloproteinase inhibitors sulphonylated amino acid hydroxamates with MMP inhibitory properties act as efficient inhibitors of

CA isozymes I, II, and IV, and N-hydroxysulphonamide inhibit both these zinc enzymes, J. Med. Chem. 43 (2000) 3677-3687.

[13] S.K. Miller, D.G. Van-Derveer, L.G. Marzilli, Models for the interaction of Zn-2+ with dna - the synthesis and x-ray structural characterization of 2 octahedral Zn complexes with monomethyl phosphate-esters of 6-oxopurine 5'-monophosphate nucleotides, J. Am. Chem. Soc. 107 (1985) 1048-1055.

[14] A.L. Nolan, M.J. McLaughlin, S.D. Mason, Chemical speciation of Zn, Cd, Cu, and Pb in pore waters of agricultural and contaminated soils using donnan dialysis, Environ. Sci. Technol. 37 (2003) 90-98.

[15] Q. Li, X.H. Zhao, Q.Z. Lv, G.G. Liu, The determination of zinc in water by flame atomic absorption spectrometry after its separation and preconcentration by malachite green loaded microcrystalline triphenylmethane, Sep. Purif. Technol. 55 (2007) 76–81.

[16] M. Hosseini, Z. Vaezi, M.R. Ganjali, F. Faridbod, S.D. Abkenar, K. Alizadeh, M. Salavati-Niasari, Fluorescence “turn-on” chemosensor for the selective detection of zinc ion based on Schiff-base derivative, Spectrochim. Acta A 75 (2010) 978-982.

[17] P. Kaur, S. Kaur, A. Mahajan, K. Singh, Highly selective colorimetric sensor for Zn^{2+} based on hetarylazo derivative, Inorg. Chem. Commun. 11 (2008) 626–629.

[18] P. Wilhartitz, S. Dreer., R. Krismer, O. Bobleter, High performance ultra-trace analysis in molybdenum and tungsten accomplished by on-line coupling of ion chromatography with simultaneous ICP-AES, Mikrochim. Acta 125 (1997) 45-52.

[19] A.R. Fakhari, M. Shamsipur, K.H. Ghanbari, Zn(II)-selective membrane electrode based on tetra(2-aminophenyl) porphyrin, Anal. Chim. Acta 460 (2002) 177–183.

[20] M.B. Gholivand, Y. Mozaffari, PVC-based bis(2-nitrophenyl)disulfide sensor for zinc ions, Talanta 59 (2003) 399-407.

[21] N.R. Gupta, S. Mittal, S. Kumar, S.K.A. Kumar, Potentiometric studies of *N*,*N*′-Bis(2-dimethylaminoethyl)-*N*,*N*′-dimethyl-9,10 anthracenedimethanamine as a chemical sensing material for Zn(II) ions, Mater. Sci. Eng. C 28 (2008) 1025-1030.

[22] V.K. Gupta, S. Agarwal , A. Jakob, H. Lang, A zinc-selective electrode based on *N*,*N*′-bis(acetylacetone)ethylenediimine, Sens. Actuators B 114 (2006) 812–818.

[23] V.K. Gupta, A.K. Jain, G. Maheswari, A new Zn^{2+}-selective potentiometric sensor based on dithizone—PVC membrane, Chem. Anal. (Warsaw) 51 (2006) 889-897.

[24] M. Hosseini, S.D. Abkenar, M.R. Ganjali, F. Faridbod, Determination of zinc(II) ions in waste water samples by a novel zinc sensor based on a new synthesized Schiff's base, Mater. Sci. Eng. C 31 (2011) 428-433.

[25] P. Singh, A.K. Singh, A.K. Jain, Electrochemical sensors for the determination of Zn^{2+} ions based on pendant armed macrocyclic ligand, Electrochim. Acta 56 (2011) 5386–5395.

[26] X. Lu, Z. Wang, Z. Geng , J. Kang, J. Gao, 2,4,6-tri(3,5-Dimethylpyrazoyl)-1,3,5-triazine modified carbon paste electrode for trace Cobalt(II) determination by differential pulse anodic stripping voltammetry, Talanta 52 (2000) 411-416.

[27] V.K. Gupta, A PVC-based 12-crown-4 membrane potentiometric sensor for zinc(II) ions, Sens Actuat B 55 (1999)195–200.

[28] V.K. Gupta, M. Al Khayat, A.K. Minocha, P. Kumar, Zinc (II) - selective sensors based on dibenzo-24-crown-8 in PVC matrix, Anal. Chim. Acta 532 (2005)153-158.

[29] S. Chandra, D.R. Singh, Zinc(II) selective poly(vinyl chloride) membrane ISE using a macrocyclic compound 1,12,14-triaza-5,8-dioxo-3(4),9(10)-dibenzoylcyclopentadeca-1,12,14-triene as neutral carrier, J. Saudi Chem. Soc. 14 (2010) 55-60.

[30] V.K. Gupta, D. K. Chauhan, V.K. Saini, S. Agarwal, M.M. Antonijevic, H. Lang, A porphyrin based potentiometric sensor for Zn^{2+} determination, Sensors 3 (2003) 223-235.

[31] V.K. Gupta, A.K. Jain, R. Mangla, P. Kumar, A new Zn^{2+}-selective sensor based on 5,10,15,20-tetraphenyl-21*H*,23*H*-porphine in PVC Matrix, Electroanalysis 13 (12) (2001) 1036–1040

[32] V.K. Gupta, A. Kumar, R. Mangla, Protoporphyrin IX dimethyl ester as active material in PVC matrix membranes for the fabrication of zinc(II) selective sensor, Sens. Actuators B 76 (2001) 617–623.

[33] A.K. Jain, S.M. Sondhi, S. Rajvanshi, A PVC based hematoporphyrin IX membrane potentiometric sensor for zinc(II), Electroanalysis 14 (2002) 293-296

[34] M. Shamsipur, S. Rouhani, M.R. Ganjali, H. Sharghi, H. Eshghi, Zinc-selective membrane potentiometric sensor based on a recently synthesized benzo-substituted macrocyclic diamide, Sens. Actuators B 59 (1999) 30–34.

[35] A.K. Singh, A.K. Jain, P. Saxena, S. Mehtab, Zn(II)-selective membrane electrode based on tetraazamacrocycle [$Bzo_2Me_2Ph_2$(16)hexaeneN_4], Electroanalysis, 18 (2006) 1186-1192.

[36] O.R. Shehab, A.M. Mansour, New thiocyanate potentiometric sensors based on sulfadimidine metal complexes: Experimental and theoretical studies, biosensors & bioelectronics 57 (2014) 77-84.

[37] Y. Umezawa, P. Buhlmann, K. Umezawa, K. Tohda, S. Amemiya, Potentiometric selectivity coefficients of ion-selective electrodes Part I. Inorganic cations - (Technical report), Pure Appl. Chem. 72 (2000) 1851–2082.

[38] E. Lindner, Y. Umezawa, Performance evaluation criteria for preparation and measurement of macro- and microfabricated ion-selective electrodes (IUPAC Technical Report), Pure Appl. Chem. 80 (2008) 85–104.

[39] N.T. Abdel Ghani, A.M. Mansour, Molecular structures of 2-arylaminomethyl-1H-benzimidazole: Spectral, electrochemical, DFT and biological studies, Spectrochim. Acta part A, 91 (2012) 272-284.

[40] T.A. Koopmans, Ordering of wave functions and energies to the individual electrons of an atom, Physica 1 (1933) 104–113.

[41] A.M. Mansour, Crystal structure, DFT, spectroscopic and biological activity evaluation of analgin complexes with Co(II), Ni(II) and Cu(II), Dalton Transactions, 43 (2014) 15950-15957.

[42] Frisch M.J., Trucks G.W., Schlegel H.B., Scuseria G.E., Robb M.A., Cheeseman J.R., Zakrzewski V.G., Montgomery J.A., Stratmann R.E., Burant J.C., Dapprich S., Millam J.M., Daniels A.D., Kudin K.N., Strain M.C., Farkas O., Tomasi J., Barone V., Cossi M., Cammi R., Mennucci B., Pomelli C., Adamo C., Clifford S., Ochterski J., Petersson G.A., Ayala P.Y., Cui Q., Morokuma K., Malick D.K., Rabuck A.D., Raghavachari K., Foresman J.B., Cioslowski J., Ortiz J.V., Baboul A.G., Stefanov B.B., Liu G., Liashenko A., Piskorz P., Komaromi I., Gomperts R., Martin R.L., Fox D.J., Keith T., Al-Laham M.A., Peng C.Y., Nanayakkara A., Gonzalez C., Challacombe M., Gill P.M.W., Johnson B.G., Chen W., Wong M.W., Andres J.L., Head-Gordon M., Replogle E.S., Pople J.A. 2003. GAUSSIAN 03 (Revision A.9), Gaussian, Inc., Pittsburgh, 2003.

[43] E. Bakker, P. Buhlmann, E. Pretsch, Carrier-Based Ion-Selective Electrodes and Bulk Optodes. 1. General Characteristics, Chem. Rev. 97 (1997) 3083-3132.

[44] V.A. Nicely, J.I. Dye, A General Purpose Curvefitting Program for Class and Research Use, J. Chem. Educ. 48 (1971) 443-448.

[45] E. Ammann, P. Pretsch, W. Simon, E. Lindner, A. Bezegh, E. Pungor, Lipophilic salts as membrane additives and their influence on the properties of macro- and micro-electrodes based on neutral carriers, Anal. Chim. Acta 171 (1985) 119–129.

[46] R. Eugster, P.M. Morf, U. Spichiger, W. Simon, Selectivity-modifying influence of anionic sites in neutral-carrier-based membrane electrodes**,** Anal. Chem. 63 (1991) 2285-2289.

[47] E.A. Cummings, P. Mailley, S. Linquette-Mailley, B.R. Eggins, E.T. McAdams, S. McFadden, Amperometric carbon paste biosensor based on plant tissue for the determination of total flavanol content in beers, Analyst 123(10) (1998) 1975-1980.

[48] R. Eugster, U.E. Spichiger, W. Simon, Membrane model for neutral-carrier-based membrane electrodes containing ionic sites, Anal. Chem. 65 (1993) 689-695.

[49] X. Yang, N. Kumar., H. Chi H., D.B. Hibbert, P.N.W. Alexandr, Lead-selective membrane electrodes based on dithiophenediazacrownether derivatives, Electroanalysis 9 (1997) 549-553.

[50] L.I. Antropov, Theoritical Electrochemistry, Mir Publisher, Moscow 1972.

[51] T. Rostzin, E. Bakker, K. Suzuki, W. Simon, Lipophilic and immobilized anionic additives in solvent polymeric membranes of cation-selective chemical sensors,, Anal. Chim. Acta 280 (1993) 197-208.

[52] S. Ishihara, K. Minami, J. Labuta, J.P. Hill, W.V. Rossom, K. Ariga , D. Ishikawa, Porphyrin-based sensor nanoarchitectonics in diverse physical detection modes, Phys. Chem. Chem. Phys., 16 (2014) 9713-9746.

[53] I. Fleming, Frontier Orbitals and Organic Chemical Reactions, Wiley, London 1976.

[54] S. Sadeghi, M. Eslahi, M.A. Naseri, H. Naeimi, H. Sharghi, A. Shameli, Copper Ion Selective Membrane Electrodes Based on Some Schiff Base Derivatives, Electroanalysis 15 (2003) 1327-1333

[55] M. Qureshi, J.P. Rawat, T. Kaur, Determination of microgram quantities of zinc by oscillometric titration with potassium ferrocyanide, J. Electroanal. Chem. 26 (1970) 409-411.

List of Figures

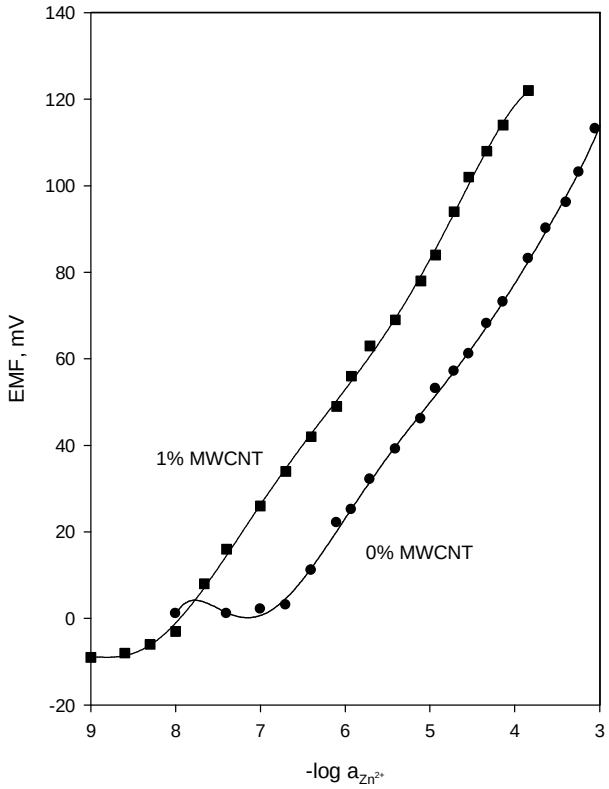

Fig. 1

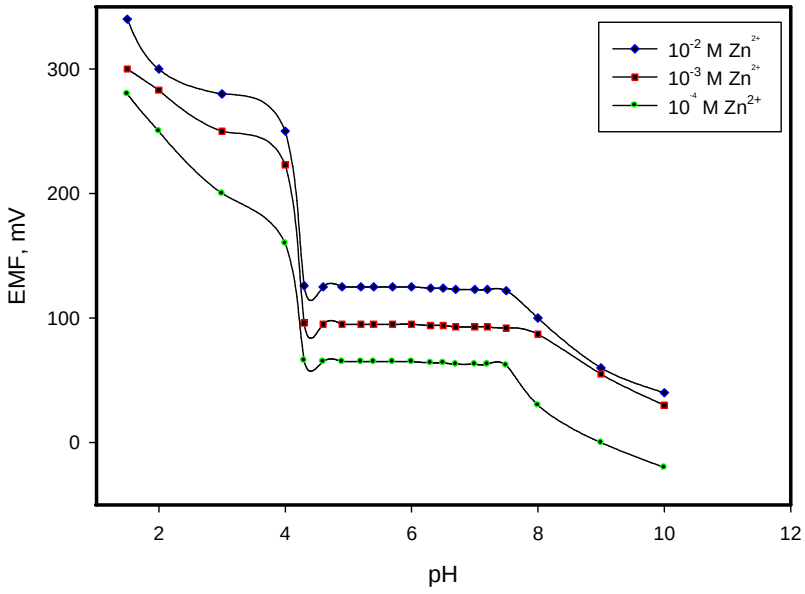

Fig. 2

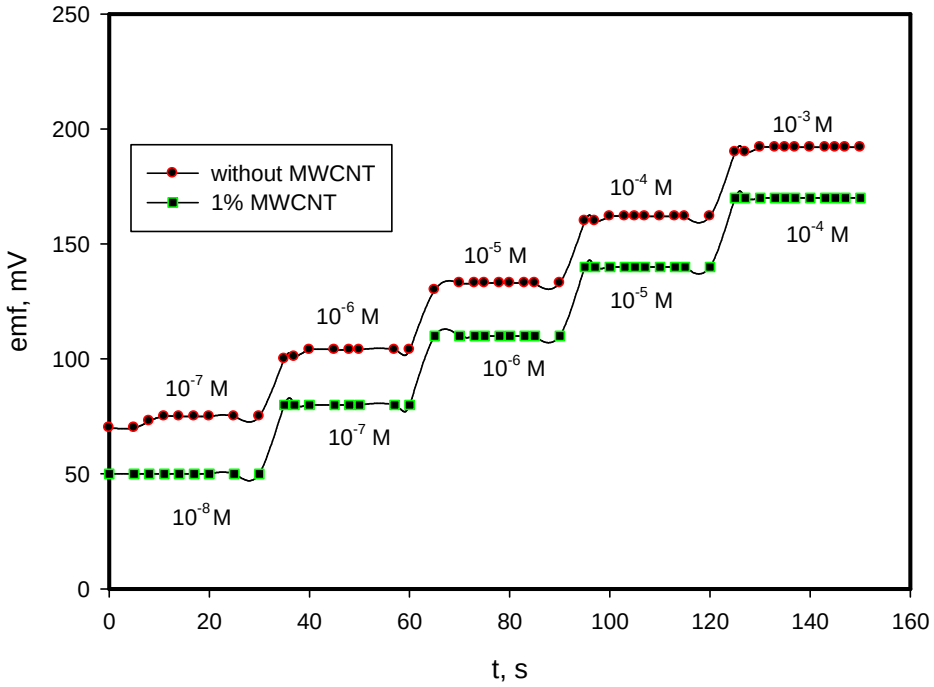

Fig. 3

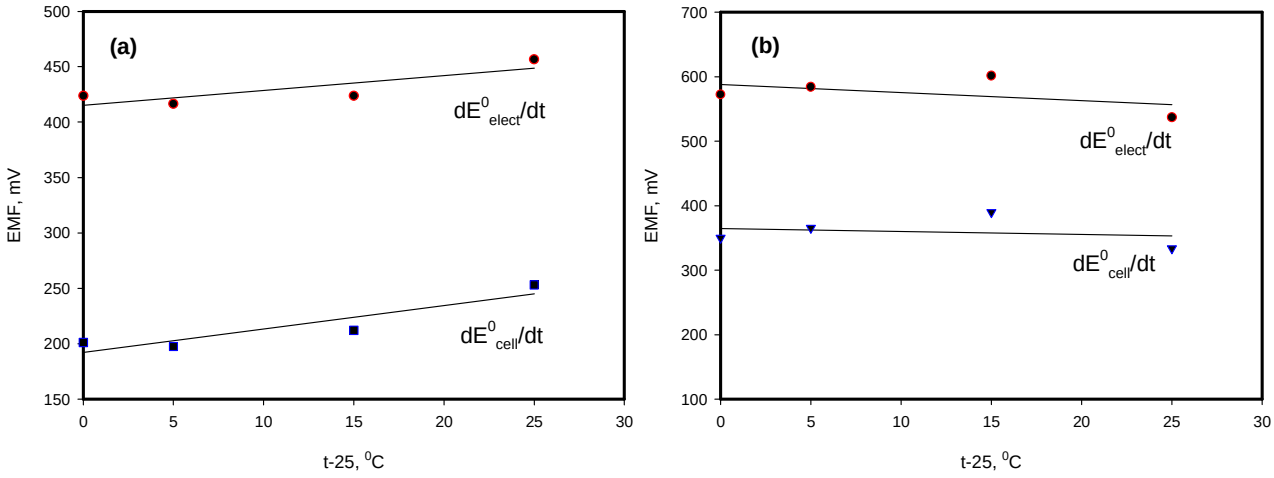

Fig. 4

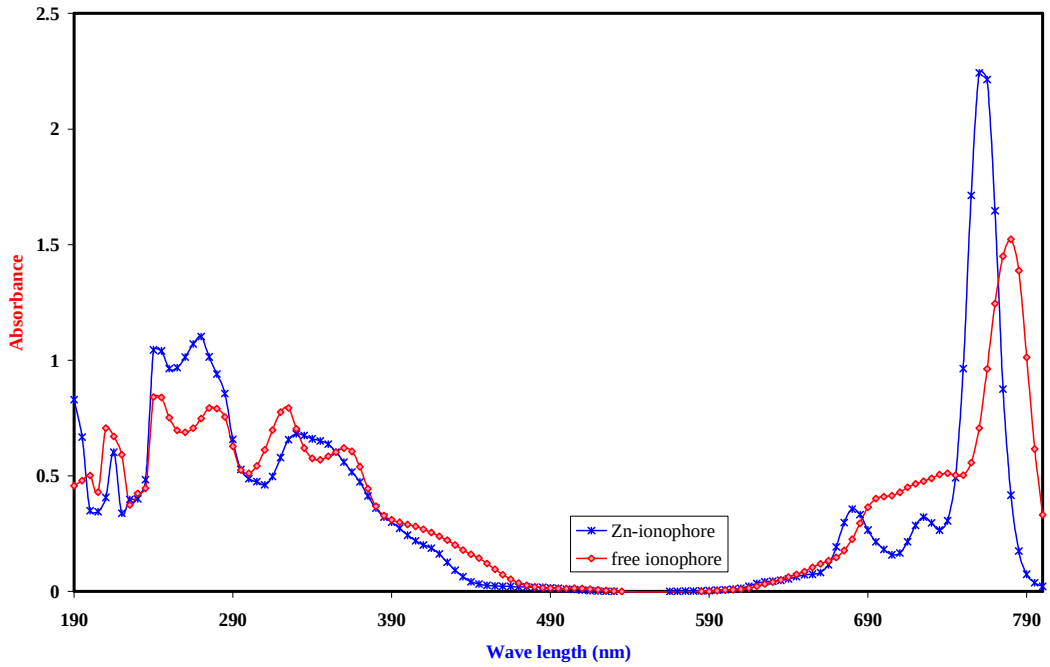

Fig. 5

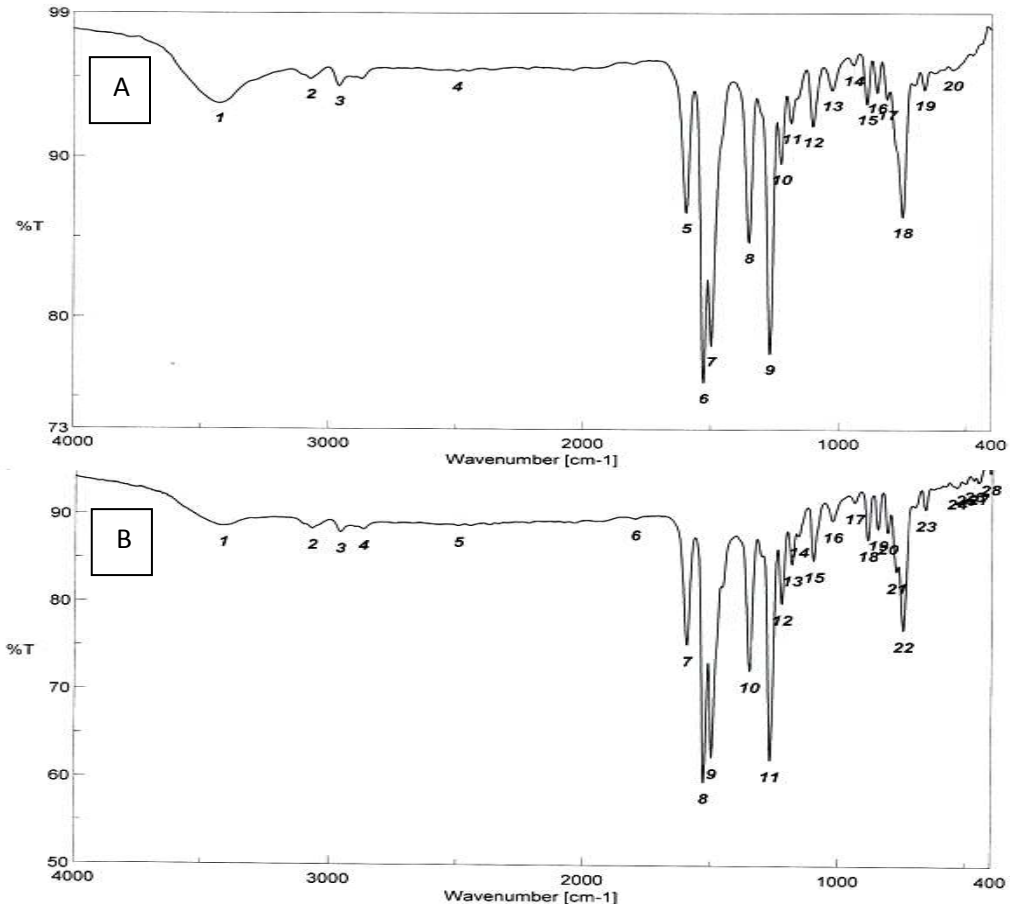

Fig. 6

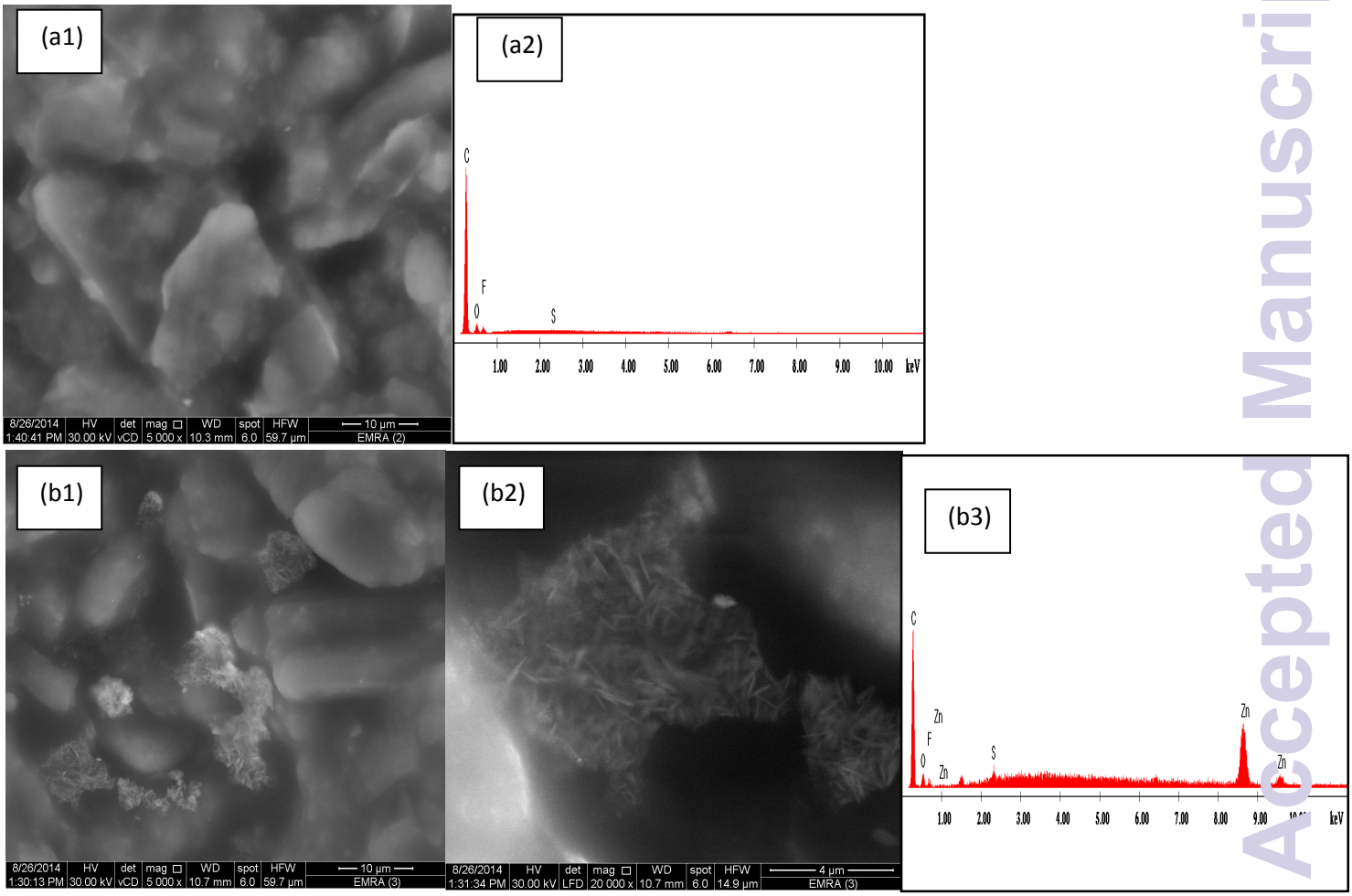

Fig. 7

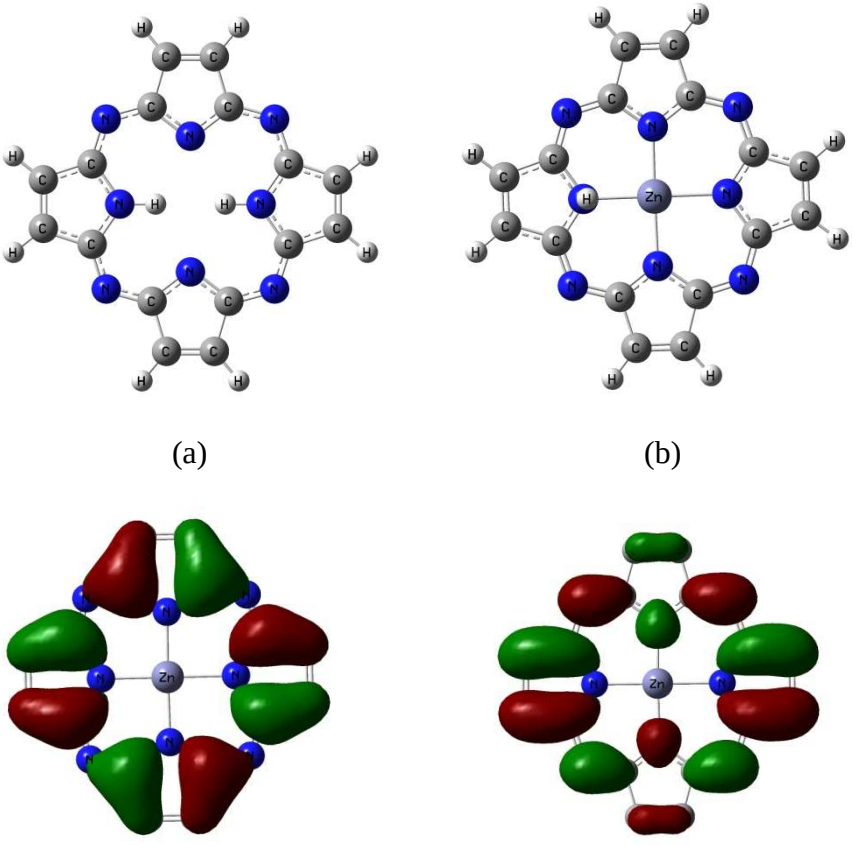

(a) (b)

(c) (d)

Fig. 8

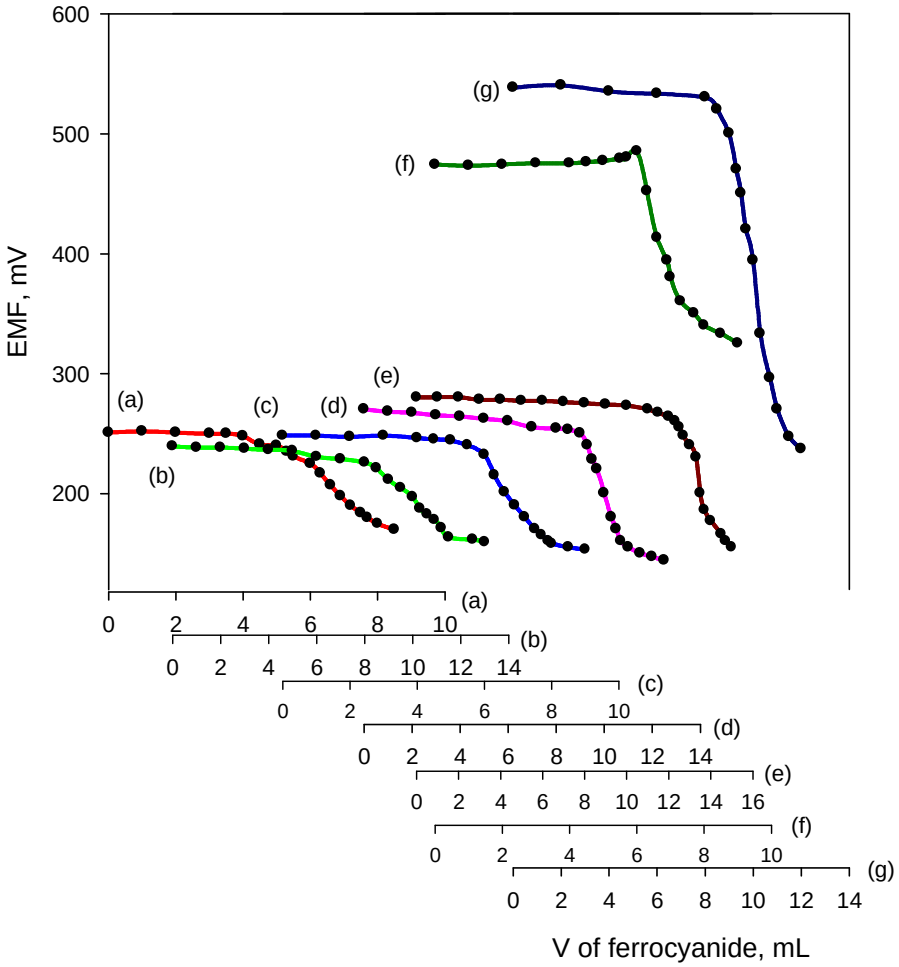

Fig. 9

Table 1: Comparison of the proposed Zn-MWCNTCP electrode with the reported electrodes

Ion-recognition	Slope, mV	Linear range, M	LOD, M	Response time, s	Ref.
5,10,15,20-Tertraphenyl-21H,23H-porphine	29.0	6.2×10^{-6}-1.0×10^{-1}	-	12	31
Tetramethyl-8,13-divinyl-2,18-porphine-dipropionic acid	30.0	1.3×10^{-5}- 1.0×10^{-1}	-	10	30
Hematoporphyrin IX	28.6	5.0×10^{-5}-1.0×10^{-1}	-	30	33
Protoporphyrin IX	29.0	1.5×10^{-5}-1.0×10^{-1}	-		32
benzo-substituted macrocyclic diamide	30.0	9.0×10^{-5}-1.0×10^{-1}	5.0×10^{-5}	20	34
Bzo2Me2Ph2(16)hexaeneN4	28.5	2.8×10^{-6}- 1.0×10^{-1}	2.2×10^{-6}	<10	35
12-crown-4	29.5	7.0×10^{-5}-1.0×10^{-1}	-	10	27
triaza-5,8-dioxo-3(4),9(10)-dibenzoyl-1,12,14-triene	29.2	1.3×10^{-7}-1.0×10^{-1}	1.0×10^{-8}	7	29
Thiazolidin-4-one	29.0	9.2×10^{-5}-1.0×10^{-2}	2.0×10^{-7}	12	28
tetra-tert-butyl-2,3-naphthalocyanine	29.9	1.0×10^{-8}-1.5×10^{-4}	5.0×10^{-9}	5	This work

Table 2: Composition and slope of calibration curves for Zn(II)-CMCPEs.

No	Ionophore	%Composition Graphite	Plasticizer	additive	Slope (mV)	linear range (M)	Detection limit (M)	Relative standard deviation %[a]
1	2	49.0	49.0 NPOE	-	43.0	2.5×10^{-4}-5.0×10^{-3}	1.60×10^{-4}	1.12
2	3	49.0	48.0 NPOE	-	55.0	3.2×10^{-4}-3.2×10^{-3}	1.00×10^{-4}	1.21
3	1	49.5	49.0 NPOE	0.5 NaTFPB	37.1	7.9×10^{-6}-3.2×10^{-3}	7.90×10^{-6}	1.45
4	2	48.5	49.0 NPOE	0.5 NaTFPB	33.2	3.9×10^{-6}-5.0×10^{-3}	3.80×10^{-6}	0.24
5	3	48.5	47.5 NPOE	0.75 NaTFPB	50.5	1.9×10^{-5}-2.5×10^{-3}	9.50×10^{-6}	0.34
6	2	48.5	49.0 NPOE	0.5 NaTImB	29.9	3.9×10^{-6}-3.9×10^{-3}	2.13×10^{-6}	0.33
7	2	48.5	49.0 NPOE	0.5 NaTPB	16.7	1.3×10^{-6}-5.0×10^{-3}	1.09×10^{-6}	2.13
8	2	48.5	49.0 DBP	0.5 NaTImB	17.6	7.9×10^{-6}-5.0×10^{-3}	5.88×10^{-6}	2.56
9	2	48.5	49.0 DOA	0.5 NaTImB	39.7	5.0×10^{-5}-1.0×10^{-2}	4.16×10^{-5}	2.44
10	2	48.5	49.0 TCP	0.5 NaTImB	24.7	1.3×10^{-6}-5.0×10^{-4}	1.25×10^{-6}	1.22
11	2	48.5	49.0 DBBP	0.5 NaTImB	55.7	1.6×10^{-4}-5.0×10^{-3}	7.94×10^{-5}	1.78
12	2	48.5	49.0 FPNPE	0.5 NaTImB	26.6	3.9×10^{-7}-5.0×10^{-3}	3.98×10^{-7}	0.66
13	2	48.0	49.0 FPNPE	1.0 NaTImB	29.3	2.0×10^{-7}-1.5×10^{-3}	2.00×10^{-7}	0.44
14	2	47.0	50.0 FPNPE	1.0 NaTImB	28.7	3.9×10^{-7}-9.3×10^{-4}	3.90×10^{-7}	0.33
15	2	46.5+0.5 M	50.0 FPNPE	1.0 NaTImB	29.47	5.0×10^{-8}-1.3×10^{-5}	5.01×10^{-8}	0.21
16	2	46.0+1.0 M	50.0 FPNPE	1.0 NaTImB	29.91	1.0×10^{-8}-1.5×10^{-4}	5.01×10^{-9}	0.23
17	2	45.5+ 1.5 M	50.0 FPNPE	1.0 NaTImB	29.50	5.0×10^{-8}-1.5×10^{-4}	1.00×10^{-8}	0.36

M: Multiwalled carbon nanotube

[a] average of four replicates.

Table 3: Performance characteristics of Zn(II)-CMCPE at different test solution temperatures.

Temperature (^{0}C)	Slope (mV/decade)		Linear range (M)	
	0% MWCNT	1% MWCNT	0% MWCNT	1% MWCNT
25	29.96	29.50	3.98×10^{-7}-1.28×10^{-2}	1.00×10^{-8}-1.47×10^{-4}
30	30.95	29.98	4.57×10^{-7}-5.49×10^{-2}	1.00×10^{-8}-1.50×10^{-4}
40	32.79	34.76	3.98×10^{-7}-1.14×10^{-2}	1.00×10^{-8}-1.00×10^{-4}
50	33.10	35.85	3.98×10^{-7}-3.54×10^{-2}	1.00×10^{-8}-1.11×10^{-4}

Table 4: Selectivity coefficient values for the proposed Zn(II)-CMCPE.

Cation	Log $K_{Znj}^{Pot.}$	
	With 1% MWCNT	Without MWCNT
Zn^{2+}	0.00	0.00
Na^{+}	-7.12	-5.00
NH_4^{+}	-6.51	-3.72
K^{+}	-7.37	-4.51
Cd^{2+}	-2.23	-1.55
Ba^{2+}	-1.35	-1.62
Ca^{2+}	-1.45	-1.71
Ni^{2+}	-1.25	-1.75
Pb^{2+}	-3.51	-0.34
Mg^{2+}	-1.18	-1.44
Mn^{2+}	-3.15	-7.65
Cu^{2+}	-2.03	0.37
Al^{3+}	-1.35	2.70
Fe^{2+}	-1.32	-0.03
Fe^{3+}	-0.76	0.37

Table 5: The calculated binding energies of several metal ions to the ligand in terms of kJ mol^{-1}

Metal ion	Binding energy
Na^{+}	-146.657
Mg^{2+}	-75.6891
Al^{3+}	-291.089
K^{+}	-392.712
Ca^{2+}	-294.171
Mn^{2+}	-65.1576
Ni^{2+}	-19.3597
Cu^{2+}	-44.4163
Zn^{2+}	-77.4744
Cd^{2+}	-454.393
Ba^{2+}	-1039.63
Pb^{2+}	-478.316

Table 6: Determination of zinc in multivitamin, eye drop, and water samples using Zn(II)-MWCNT-CPE

	Found (µg/mL)		Recovery%	Relative standard deviation %[a]
	Potentimetrically	AAS		
Mammy Vit	24.60	25.00	98.40	1.33
Eye drop	70.11	70.48	99.47	1.11
Tap water	2.09	2.14	97.80	1.66
Waste water	0.68	0.66	102.40	1.32
Pure samples	Taken (µg/mL)	Found (µg/mL)		
	0.49	0.50	98.00	1.02
	0.98	1.00	98.00	1.12
	2.99	3.00	99.60	1.04
	4.99	5.00	99.80	1.10

[a] average of four replicates.

Table 7: Potentiometric titration for determination of zinc in pure solution using Zn(II)-MWCNT-CPE

Taken (µg/mL)	Found (µg/mL)	R	RSD	Jump, mV
6.50	6.51	100.15	1.34	45
9.75	9.65	98.97	1.21	65
65.00	64.74	99.60	1.22	80
97.50	96.40	99.38	1.12	95
130.00	129.90	99.92	1.01	100
650.00	641.50	98.69	1.00	125
975.00	970.10	99.49	1.45	230